Capillary Rise in Granitic Rocks: Interpretation of Kinetics on the Basis of Pore Structure

María J. Mosquera,*,[1] Teresa Rivas,† Beatriz Prieto,† and Benita Silva†

Departamento de Química-Física, Facultad de Ciencias, Universidad de Cádiz, Puerto Real (Cadiz), Spain; and †Departamento de Edafología, Universidad de Santiago de Compostela, Santiago de Compostela, Spain

The capillary transport of water into granitic rocks has been interpreted on the basis of the structure of its porous network. An effective pore radius has been calculated from a three-sized single-pore model proposed by F. A. L. Dullien, El-Sayed, and V. K. Batra (*J. Colloid Interface Sci.* **60, 497, 1977**) Considering the porous network of granites as consisting of fissures grouped in two size types, macro- and microfissures, an effective radius was found from the characteristic radii for each type and the average of these two values. Good agreement between the effective radius calculated and the radius estimated using a capillary rate value measured experimentally provides a suitable basis for identifying interrelationships between the pore structure and moisture capillary rise. In fact, it is possible to predict the process rate from only two characteristic pore sizes, corresponding to the radii of macrofissures and microfissures. The abnormally low rate of capillary rise observed in one of the granites studied could be easily interpreted as due to the involvement exclusively of the macrofissures of its porous network in capillary transport.   © 2000 Academic Press

Key Words: capillary rise; granites; kinetic interpretation; pore size distribution.

INTRODUCTION

The decay of many stone buildings and monuments is induced by diverse processes in which water plays a major role, in one form or another: dissolution and swelling of stone minerals, growth of biological species, internal stress due to water freezing, crystallization and hydration of salts, and others. Therefore the study of moisture transport into the stone of buildings, such as water rise thorough the material's porous network, is of particular importance. In the specific case of granitic rocks with a homogeneous and well-interconnected porous system, the study of this kind of moisture transport is particularly interesting in understanding the process of damage and the correct selection of conservation treatments. Specifically, the prediction of the effect on capillary transport caused by the closure of pores by consol-

idation agents used in these treatments is clearly of practical importance.

In particular, it is important to identify the interrelationship between kinetic processes and stone pore network, since porous structure is one of the main parameters controlling this transport. In the literature, however, there are only a few studies on the kinetics of the process, and these are dedicated exclusively to sedimentary rocks. In most of them, water capillary rise is described according to the Washburn equation (1), which establishes a linear relationship between the height of the rise and the square root of time when the gravity effect can be neglected:

$$h = \sqrt{\frac{\gamma \cdot \cos\theta \cdot r}{2\mu}t},\qquad [1]$$

where γ is water surface tension, θ is contact angle of water–solid, μ is fluid viscosity, and r is pore radius. Obviously, the capillary pressure head is much greater than the hydrostatic pressure head for laboratory-scale samples; therefore, the gravity effect can be discounted. The exponential model suggested by other authors (2), dealing exclusively with capillary rise where the gravity effect is substantial, has already been discussed in an earlier paper (3).

The main deficiency of this model, as can be concluded from Eq. [1], is the fact that only a single cylindrical capillary is used to characterize a network of interconnected capillaries of varying radius. The practical consequence of this assumption is that the effective pore radius calculated using the Washburn equation is one or two orders of magnitude smaller than the smallest pore in the network. As pointed by Dullien *et al.* (4), this discrepancy can be explained as follows: the water spends the majority of time in the largest pores where the capillary driving force is lowest and the volume to be filled is greatest. The relatively long time spent in the largest segments results in abnormally low rates of capillary rise, and is responsible for the small values of effective pore radius calculated by the Washburn equation.

With the aim of resolving this inconvenience, Dullien *et al.* (4) developed a new model for a three-dimensional pore structure consisting of a repeating pore element with step changes in its diameter. The theoretical expression obtained for the effective

[1] To whom correspondence should be addressed. E-mail: mariajesus. mosquera@uca.es. Fax: 34(56)016288.

pore diameter is

$$D_{\text{eff}} = \frac{1}{3} \left[\sum_k D_k \right]^2 \left[\sum_k D_k \sum_j \left(\frac{D_k}{D_j} \right)^3 \right]^{-1}, \qquad [2]$$

where the summations are over the number of segments of the repeating pore unit.

The porous network structure of sedimentary rocks contains a large proportion of "ink-bottle" pores with different neck and bulge radii. Therefore, Dullien *et al.* used three characteristic pore sizes for the model: the maximum pore size measured by microscopy, the pore size at the inflection point on a mercury porosimetry curve corresponding to pore entry, and the average of these two values. The effective pore diameter calculated was much smaller than the individual units of the pore segments, showing considerable similarity with the diameter calculated by the Washburn equation in a wide variety of sandstone samples. Recently, Einset (5) satisfactorily applied the model to the process of capillary infiltration of silicon into a carbonaceous material. Again, the predicted values are consistent with the measured data.

The objective of this paper is to study the kinetics of water capillary rise in granitic rocks and to determine the influence of the porous network structure of stone on the process. The Dullien model is used with a variety of granitic rocks that were characterized by mercury porosimetry and fluorescence microscopy. Considering the significant differences in pore structure between granites and sedimentary rocks, new criteria for selection of characteristic pore size are developed.

STONE MATERIALS AND CHARACTERISATION

Three granitic rocks—Baleante, Roan, and Axeitos—used extensively in monumental construction in Galicia (northwest Spain), were selected for this study.

Baleante is a medium-coarse-grained muscovite-rich leucogranite with abundant xenoliths and with an evident mineral orientation marked by the mica crystals. Roan is a fined-grained two-mica granite with panallotriomorphic equigranular texture, signs of flow structure, and xenoliths. Finally, Axeitos is a slightly pinkish coarse-grained posthercynian granite, with an allotriomorphic-to-subidiomorphic heterogranular texture and without apparent mineral orientation (6).

The following tests were carried out on specimens taken of sound rocks:

• Fluorescence microscopy of thin sections (FM): The porous structure of granitic rocks was investigated by means of fluorescence optical microscopy, using polished thin sections impregnated with a fluorescent resin (Rodamina B).

• Open porosity test: the porosity accessible to water was determined by means of the RILEM Procedure (7) for five 5-cm cubic samples of each type. The porosity determination is essentially very simple: the specimen mass, dried until of constant weight, is measured (m_d). Then it is placed under vacuum and immersed in distilled water until all open pores are completely filled with water. Then its mass is measured both under water (m_w) and normally in air (m_m). Using Archimedes' law, the open porosity can be found from

$$P(\%) = \frac{m_m - m_d}{m_m - m_w} \cdot 100. \qquad [3]$$

• Mercury intrusion porosimetry (MIP): The MIP measurements were carried out with both a low-pressure (up to 400 kPa) and a high-pressure (max 400 MPa) porosimeter (Pascal, Fision Instruments). This enables the measurement of pores with a radius range between 2.5 nm and 58 μm. The specimens, with an average size of 2 cm^3, were previously cleaned in a microwave bath and dried at 60°C.

• Capillary rising test: This was performed according to the RILEM Procedure (8) for five 5-cm cubic samples of each of the granite types. The specimens, previously dried, are placed in a tank containing distilled water to a depth of approximately 2 mm. The variation of the mass of water absorbed is monitored at regular intervals of time. Given the anisotropy of granitic rocks, the capillary rising test was performed in three orthogonal sample orientations. To minimize the tortuosity factor, we decided to use the data corresponding to the highest absorption result.

EXPERIMENTAL RESULTS

Fluorescence microscopy of thin sections showed the porosity of the rocks to consist of three kinds of fissures (Fig. 1): transgranular (fissures that cut across a grain boundary), intergranular (between grains, mainly quartz–quartz and quartz–feldspar contacts), and intragranular (within grains, mainly in plagioclase and mica crystals). On the other hand, all the fissures exhibited similar morphology with a practically uniform width along fissure length. Comparing the three selected granites, Axeitos presented a high transgranular fissuration with the highest fissure radius (40 μm). Roan and Baleante showed all three kinds of fissuration: transgranular, intergranular, and intragranular. The maximum fissure radius of Baleante was higher (25 μm) than that of Roan (10 μm).

The pore data of the selected materials are summarized in Table 1 and pore size distribution curves obtained by MIP are shown in Fig. 2. The three granites showed close porosity values (from 1.5 to 2.8%) which are characteristic of granitic rocks. Moreover, the total porosity values obtained by mercury porosimetry were consistent with those obtained by water saturation (Rilem Procedure), indicating the reliability of MIP results. In the light of the good agreement between test results, the following propositions for the application of this technique to the characterization of granite pore space can be developed:

In mercury porosimetry, the pore size distribution is often obtained according to the radii calculated with the Washburn equation (9), relating to the circular cross-section pore model. Given the different morphology of granite fissures with respect
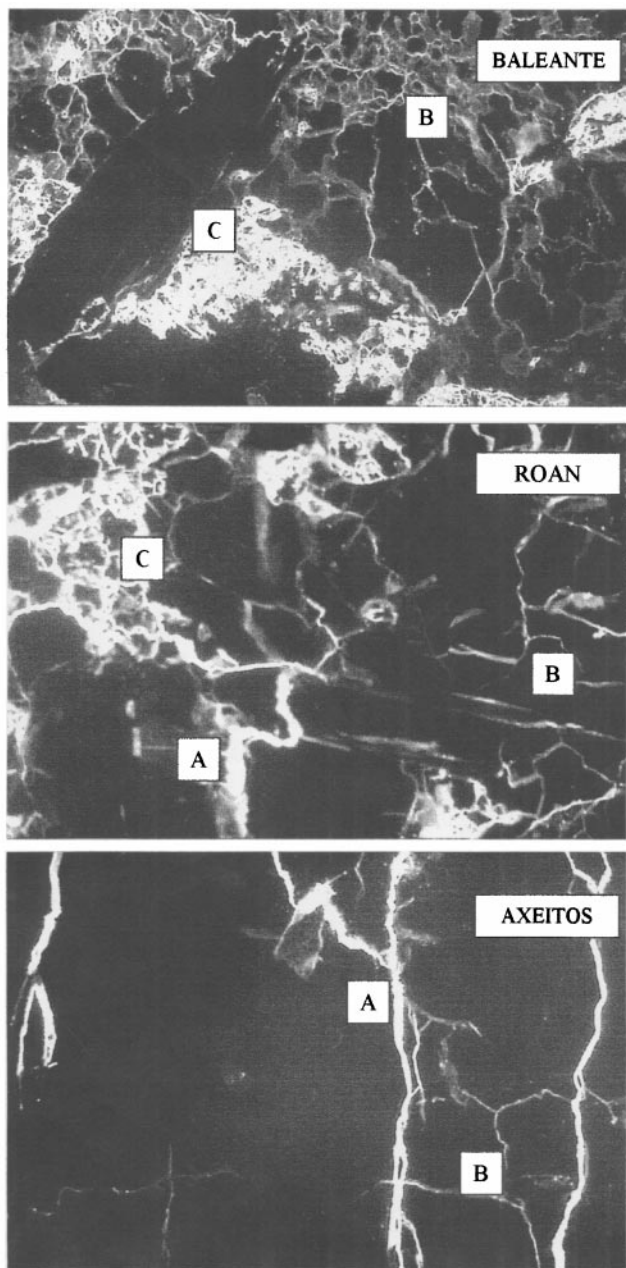
FIG. 1. Microphotographs taken under fluorescence microscopy of the granites studied. The three kinds of fissure observed are indicated by different letters, where (A) corresponds to transgranular, (B) to intergranular, and (C) to intragranular fissuration.

TABLE 1
Comparison of Porosity Data Obtained by Different Methods

	Method	Baleante	Roan	Axeitos
Porosity (vol%)	RILEM	2.78	2.11	1.94
Porosity (vol%)	MIP	2.80	2.10	1.50
Maximum radii (μm)	FM	25	10	40
Macrofissure radius range (μm)	MIP	58–1.75 (40%)[a]	58–1.75 (43%)	58–1.75 (90%)
Microfissure radius range (μm)	MIP	1.30–0.01 (60%)	0.70–0.03 (57%)	0.013–0.002 (10%)

[a] The percentage of pores corresponding to each fissure size range is given in parentheses.

section model, taking the smallest dimension of each crack as the diameter of a cylindrical pore.

Furthermore, the serious limitations found by using this technique for materials with a large proportion of "ink-bottle" pores, as with many sedimentary rocks, are eliminated in the case of granitic rocks. It is recognized that in materials with pores in the form of necks and bulges, the pore size distribution actually corresponds to the entry radii of pores, since it is mainly the constrictions that determine the resistance to mercury flow when pressure is applied. Thus, in the case of granite specimens consisting of fissures with an approximately uniform width (Fig. 1), good reliability of pore radius distribution in a MIP analysis is expected.

In fact, the pore distributions obtained by MIP correspond well with fluorescence microscopy observations. Although the mineral structure reveals three fissure types, the pore radius distribution is clearly bimodal, with macrofissures corresponding to the first linear segment in the intrusion curve and microfissures to the second segment (Fig. 2). Comparing the MIP and fluorescence microscopy observations (Fig. 1), we assumed that
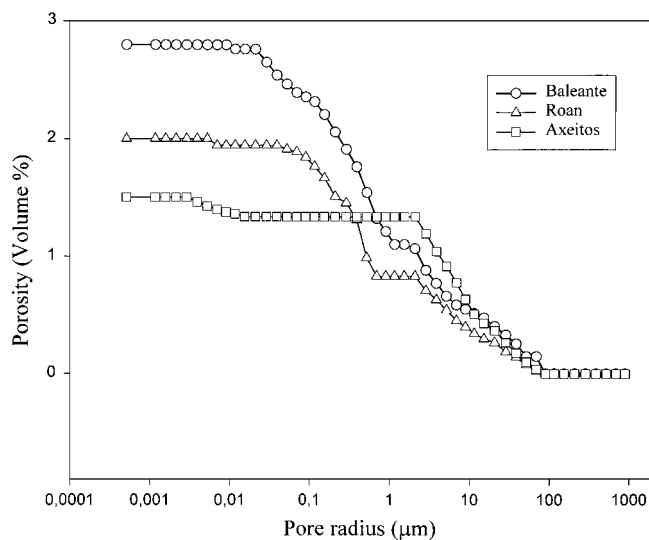
to a cylindrical form, other models with a rectangular or elliptical cross-section of pores, which conform more closely to the morphology of the granitic porous network (10, 11), have been proposed. However, the results obtained from a recent study comparing the three models showed the pore size distribution from the elliptical and rectangular models to be similar to that obtained from the circular model (11). Thus, although the rectangular model is most representative of the geometric form of a crack in granite, in this study we have used the circular cross-

FIG. 2. Pore radius distribution curves obtained by mercury intrusion porosimetry of the granites studied.
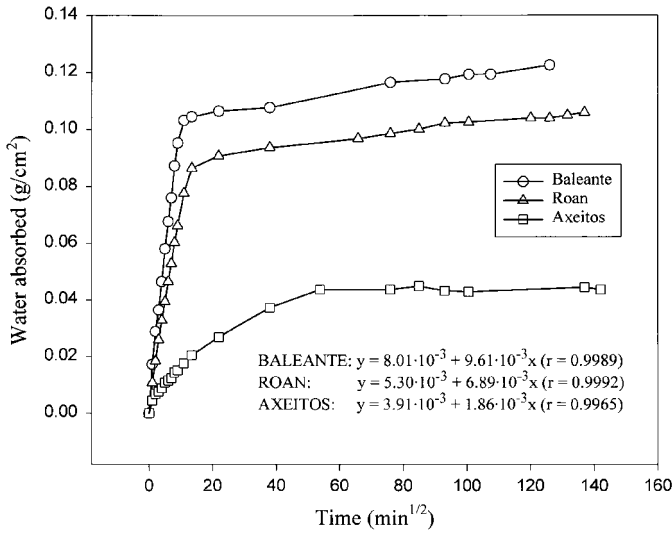
FIG. 3. Profiles of capillary rise of water in the granites selected. The linear regression equations are included.

macrofissures are the transgranular fissures while inter- and intragranular microcracks with a similar radius correspond to the microfissures.

The only discrepancy between the two techniques is with respect to the maximum radius of fissures, the MIP values being higher than those values from microscopy. The fact that the MIP data are largely independent of rock type (58 μm for all three granites) seems to suggest that microscopic investigation is more reliable. In fact, Hellmuth *et al.* (12) suggested that those macropores shown by MIP and not observed by microscopy were mostly artifacts induced by the pretreatment (basically by the sawing of specimens).

Comparing the three granitic rocks, the macrogranular fissures exhibit a similar fissure size range, while in the case of the microfissures, Axeitos granite shows a lower size range (Table 1). Moreover, the proportion of macrofissures in Axeitos is significantly higher (90% of total porosity) than in the others (40%).

The measurements of water absorbed versus time are shown in Fig. 3. Obviously, the stationary-phase corresponds to satura-

TABLE 2
Summary of Results

	Baleante	Roan	Axeitos
Capillary rate (g cm^{-2} · s$^{-1/2}$) · (10^3)	1.24	0.89	0.24
Water saturation (%)	1.05	0.77	0.44
Capillary porosity (vol%)	2.72	2.02	1.13
Washburn radius (nm)	5.78	5.32	1.24
Dullien radius (nm)	5.74	4.67	1.52

Note. Washburn radius was estimated from the experimental capillary rise measurements, using the model square root of time dependence proposed by Washburn. Dullien radius was calculated from characteristic radii of each kind of fissure obtained by fluorescence microscopy and MIP, using the three-sized single-pore model proposed by Dullien.

tion of the specimen. The first phase corresponding to the one-dimensional water rise does indeed follow the expected square root-time-dependent kinetics, as discussed in the Introduction. As seen in Fig. 3, excellent fits to this model were achieved, as indicated by the high correlation coefficients ($r > 0.99$). The values of capillary rate, which is the slope obtained in the linear regression, and saturation water content are summarized in Table 2. The most striking result is the much slower capillary rate for Axeitos granite.

INTERPRETATION OF THE RESULTS AND CONCLUSIONS

The interrelationships between pore structure and the kinetics of the capillary rise process for the granitic rocks selected have been analyzed using the theoretical model described in the Introduction. The kinetics of capillary rise in granitic rocks was interpreted in terms of single effective capillary radius, because of the complexity of their porous network structure.

First, an effective radius for each of the granite types was calculated by the Washburn equation (Eq. [1]), using the values for rates of capillary rise listed in Table 1. Since it is very difficult to measure with accuracy by visual observation the rate of the capillary fringe rise, the rates have been measured from the increase in water mass over time. To apply the Washburn model, the relationship between mass and height of water in the capillaries can easily be derived from the density definition:

$$\rho = \frac{m}{V} = \frac{m}{S \cdot h}, \qquad [4]$$

where ρ is water density, m is water mass, V is water volume, S is water surface, and h is the height of water rise.

It is evident that the surface occupied by water corresponds to the surface of the capillaries constituting the porous network, which can be calculated as the total specimen surface (S) corrected by the material porosity (P). Therefore, Eq. [1] could be rewritten as

$$\frac{m}{S} = \sqrt{\frac{\gamma \cdot \cos\theta \cdot r}{2\mu}} \cdot \rho \cdot P\sqrt{t}. \qquad [5]$$

The contact angle was assumed to be $0°$. Also, it should be noted that the air entrained in larger pores during capillary absorption could lead to serious differences between the real pore volume involved in the process and the material porosity estimated by the open porosity test, where the specimens are tested under vacuum. The porosity employed in Eq. [5] was, therefore, calculated from the quantity of water absorbed in the saturation phase of the capillary absorption process. The good agreement between capillary porosity (Table 2) and open porosity (Table 1) for Baleante and Roan granites suggests that almost all the fractions of pore radius of these rocks (98 and 95%, respectively) are involved in the capillary process. It is apparent that the differences in these parameters for Axeitos (only 58% of pores

are involved in capillary absorption) are due to the larger size of its fissures.

The effective radius values obtained, summarized in Table 2, were several orders of magnitude smaller than the radii of the narrowest fissures listed in Table 1. This is consistent with observations of Dullien *et al.* (4). It should be noted that the values for Baleante and Roan are similar (around 5 nm), while Axeitos granite has a substantially lower value (1.24 nm), which is related to its lower rate of capillary rise.

In a second stage, the effective radii were calculated from pore structure data obtained by fluorescence microscopy and MIP, using Eq. [2]. The porous network model used for sedimentary rocks consisting of a three-size single-capillary repeating unit corresponding to pores with bulge and neck is not appropriate for granitic rocks consisting of a network formed by fissures clearly grouped into two size types (macro- and microfissures) with a practically uniform width. Thus, we propose a new selection criterion in which the values for maximum and minimum radii to be used in Eq. [2] correspond to the macro- and microfissure radii. Hence the lower limit of radius employed was found from the breakthrough point at the second segment in the cumulative mercury intrusion curve corresponding to maximum radius of microfissures. In contrast, the upper limit was the median radius of macrofissures, obtained from the maximum value observed by microscopy and the minimum radius estimated by MIP. The reason for taking an average radius to use in the calculation is that most of the water rising in the larger macrofissures is lost to the neighboring narrower fissures, which make up much of the porous network.

Since practically all the pore volume of Axeitos consists of pores in the macrofissures range (90%) and, moreover, the microfissures size range is below 0.1 μm, which is not relevant in capillary transport (13), the macrofissure radii exclusively were used in the calculation.

The effective radii calculated from fissure radii showed, in all the cases, good agreement with the radii estimated by the Washburn equation (Table 2). The most striking result is that

the lower effective radius of Axeitos granite derived from its abnormally low rate of capillary rise can now be explained easily as the result of its particular fissure size distribution (microfissures are not involved in the capillary rise).

In conclusion, the agreement in the results indicates that the characterization of water capillary transport in granitic rocks is feasible by estimating only two characteristic pore sizes corresponding to the radii of the macro- and microfissures. In fact, the effect of size distribution of porous network in the rate of capillary rise has been perfectly analyzed.

Lastly it is shown in this paper that the characterization of pore size distribution in granitic rocks by mercury porosimetry is sufficient to predict capillary transport kinetics with acceptable accuracy. However, more research is needed to quantify the maximum pore size more accurately so that this parameter can be reliably measured by this procedure.

REFERENCES

1. Washburn, E. W., *Am. Phys. Soc. 2nd Ser.* **17,** 374 (1921).
2. Hoffman, D., Niesel, K., and Wagner, A., *Am. Ceram. Soc. Bull.* **69,** 392 (1990).
3. Mosquera, M. J., Alcántara, R., and Martín, *J. Am. Ceram. Soc. Bull.* **77,** 76 (1998).
4. Dullien, F. A. L., El-Sayed, and Batra, V. K., *J. Colloid Interface Sci.* **60,** 497 (1977).
5. Einset, E. O., *J. Am. Ceram. Soc.* **79,** 333 (1996).
6. Rivas, T., *in* 'Mecanismos de alteración en rocas graníticas utilizadas en la construcción de edificios antiguos en Galicia." doctoral thesis, Universidad de Santiago de Compostela, 1996.
7. RILEM, Test No. I.1: Porosité accesible à l'eau." *Mater. Construct.* **13**(75) (1980).
8. RILEM, Test No. II.6: "Coefficient d'absorption d'eau (Capillarité)." *Mater. Construct.* **13**(75), 208 (1980).
9. Washburn, E. W., *Proc. Nat. Acad. Sci. USA* **7,** 115 (1921).
10. Jenkins, R. G., and Rao, M. B., *Powder Technol.* **38,** 177 (1984).
11. Couchot, P., Dubois, C., Boeglin, E., and Chambaudet, A., *Spec. Publ. R. Soc. Chem.*, 213 (Characterisation of Porous Solid IV), 382 (1997).
12. Hellmuth, K. H., Klobes, P., Meyer, K., Röhl-Kuhn, B., Siitar-Kauppi, J., Hartikainen, and Timonen, J., *Z. Geol. Wiss.* **23,** 691 (1995).
13. Meng, B., *Mater. Struct.* **27,** 125 (1994).